

Dihedral ψ Angle Dependence of the Amide III Vibration: A Uniquely Sensitive UV Resonance Raman Secondary Structural Probe

Sanford A. Asher,^{*,†} Anatoli Ianoul,[†] Guido Mix,^{†,‡} Mary N. Boyden,[†] Anton Karnoup,[§] Max Diem,^{||} and Reinhard Schweitzer-Stenner[⊥]

Contribution from the Department of Chemistry, University of Pittsburgh, Pittsburgh, Pennsylvania 15260, Institut für Experimentelle Physik, Universität Bremen, 28359 Bremen, Germany, the Department of Chemistry, City University of New York, Hunter College, New York 10021, and the Department of Chemistry, University of Puerto Rico, Rio Piedras Campus, P.O. Box 23346, San Juan, Puerto Rico 00931-3346

Received November 15, 2000. Revised Manuscript Received August 30, 2001

Abstract: UV resonance Raman studies of peptide and protein secondary structure demonstrate an extraordinary sensitivity of the amide III (Am III) vibration and the C α H bending vibration to the amide backbone conformation. We demonstrate that this sensitivity results from a Ramachandran dihedral ψ angle dependent coupling of the amide N–H motion to (C)C α H motion, which results in a ψ dependent mixing of the Am III and the (C)C α H bending motions. The vibrations are intimately mixed at $\psi \sim 120^\circ$, which is associated with both the β -sheet conformation and random coil conformations. In contrast, these motions are essentially unmixed for the α -helix conformation where $\psi \sim -60^\circ$. Theoretical calculations demonstrate a sinusoidal dependence of this mixing on the ψ angle and a linear dependence on the distance separating the N–H and (C)C α H hydrogens. Our results explain the Am III frequency dependence on conformation as well as the resonance Raman enhancement mechanism for the (C)C α H bending UV Raman band. These results may in the future help us extract amide ψ angles from measured UV resonance Raman spectra.

Introduction

Advances in the understanding of protein structure and dynamics require development of more incisive probes. Obviously, X-ray diffraction is the gold standard of structural probes.^{1–3} Its main use is to determine static structures of hydrated solid crystals of peptides and proteins. These static X-ray structures give detailed information on conformation, bond lengths, and interresidue atomic distances.^{1–3} Protein dynamical insight, in general, can only be obtained by extrapolation between protein X-ray static structures. This is because kinetic X-ray diffraction studies are extremely rare and have been reported for just a few favorable cases.⁴

Multidimensional NMR measurements also give detailed information on protein structure in concentrated solutions.^{5,6} Unfortunately, NMR is only able to probe protein dynamics at relatively long time scales. Other structural methods, such as CD, IR absorption, Raman, and fluorescence give less complete information on protein structure, but these methods can be

utilized to study very short time peptide and protein dynamics (picosecond–microsecond) in dilute aqueous solutions.^{7–12}

CD, IR absorption, resonance Raman, and fluorescence energy transfer can be used statically, as well as dynamically (in the nanosecond time regime), to detail the first steps in protein folding and unfolding.^{7–12} For example, a recent transient synchrotron CD measurement probed the dynamics of peptide α -helix folding and unfolding.⁷ Recent fluorescence energy transfer measurements between chromophores at the end of a peptide probed the first steps in peptide α -helix formation.⁸ In addition, transient aromatic amino acid fluorescence measurements have been used to examine the evolution of the environment of these residues after a laser induced T-jump, which induced protein folding and unfolding.⁹

More recently, transient IR absorption spectroscopy examined the nanosecond time dependence of the amide I (Am I) IR absorption spectrum, which was used to monitor the first steps in the structural evolution after a T-jump.¹⁰ Most recently, our group demonstrated the utility of UV resonance Raman spectroscopy to probe protein and peptide secondary structure as well as to probe the nanosecond evolution of these structures in response to T-jumps.^{11,12}

* To whom all correspondence should be addressed. Phone: 412-624-8570. Fax: 412-624-0588. E-mail: asher+@pitt.edu.

[†] University of Pittsburgh.

[‡] Universität Bremen.

[§] Present address: The Dow Chemical Company, Midland, Michigan 48642.

^{||} City University of New York, Hunter College.

[⊥] University of Puerto Rico.

(1) *Methods in Enzymology*; Wyckoff, H. W., Hirs, C. H. W., Timasheff, S. N., Eds.; Academic Press: San Diego, CA, 1985; Vol. 114, pp 1–588.

(2) Hess, G. P.; Rupley, J. A. *Annu. Rev. Biochem.* **1971**, *40*, 1013–1044.

(3) Dickerson, R. E. *Annu. Rev. Biochem.* **1972**, *41*, 815–842.

(4) Moffat, K. *Acta Crystallogr. A* **1998**, *54*, 833–841.

(5) Billeter, M. *Q. Rev. Biophys.* **1992**, *25*, 325–377.

(6) Wüthrich, K. *Acta Crystallogr.* **1995**, *51*, 249–270.

(7) Clarke, D. T.; Doig, A. J.; Stapley, B. J.; Jones, G. R. *Proc. Natl. Acad. Sci. U.S.A.* **1999**, *96*, 7232–7237.

(8) Thompson, P. A.; Eaton, W. A.; Hofrichter, J. *Biochemistry* **1997**, *36*, 9200–9210.

(9) Thompson, P. A.; Munoz, V.; Jas, G. S.; Henry, E. R.; Eaton, W. A.; Hofrichter, J. *J. Phys. Chem. B* **2000**, *104*, 378–389.

(10) Williams, S.; Causgrove, T.; Gilmanshin, R.; Fang, K.; Callender, R.; Woodruff, W.; Dyer, R. B. *Biochemistry* **1996**, *35*, 691–697.

(11) Lednev, I. K.; Karnoup, A. S.; Sparrow, M. C.; Asher, S. A. *J. Am. Chem. Soc.* **1999**, *121*, 4076–4077.

(12) Lednev, I. K.; Karnoup, A. S.; Sparrow, M. C.; Asher, S. A. *J. Am. Chem. Soc.* **1999**, *121*, 8074–8086.

UV resonance Raman spectra excited within the amide $\pi \rightarrow \pi^*$ transitions have significantly more information content than that which occurs in CD, IR, and fluorescence.^{11–16} The spectra show numerous Raman bands from vibrational modes localized within the amide fragments of the peptide or protein. Each of these bands shows unique spectral dependencies on conformation.¹³ These differential dependencies result from the different atomic displacement coordinates within each vibration and the unique responses of each of these displacements to changes in the amide backbone conformation and hydrogen bonding.^{13–16}

In the work here, we elucidate the physical origin of the frequency and the resonance Raman enhancement dependence of the Am III and the $C_{\alpha}H$ bending modes on the peptide secondary structure. These vibrations are clearly the most structure sensitive of the amide backbone vibrational modes. We find that the normal mode composition and the mixing between the Am III vibration and the $(C)C_{\alpha}H$ bending motion is mainly determined by the amide dihedral ψ angle, as was proposed almost 25 years ago by Lord.¹⁷ We demonstrate here that the ψ angle dependence results from a ψ angle dependent coupling between $(C)C_{\alpha}H$ and N–H bending motions. The importance of this result is that, if we can determine the frequencies and enhancement patterns of the Am III and the $(C)C_{\alpha}H$ bending vibrations of an amide linkage in a peptide, then we may be able in the future to determine its ψ angle.

Materials and Methods

Materials. *N*-Methylacetamide ($CH_3CONHCH_3$, NMA) was purchased from Aldrich Chemical Co. Alanine (A_3), tetraalanine (A_4), and glycine methylamide ($NH_3CH_2CONHCH_3$, ANMA) were obtained from Bachem Bioscience Inc. *N*-Acetyl-D-alanine ($CH_3CONHCH_2COOH$, AcA), *N*-acetyl glycine ($CH_3CONHCH_2COOH$, AcG), diglycine (GG), pentaalanine (A_5), polyglutamic acid (PGA), lysozyme, and myoglobin were purchased from Sigma Chemical Co. Triglycine (G_3) and *N*-acetyl glutamic acid (AcE) were purchased from ICN Biomedicals Inc. All commercial purchased compounds were used without further purification.

The alanine based polypeptide (AP) of composition $A_5(A_3RA)_3A$ was synthesized (>95% purity) at the Pittsburgh Cancer Institute by the solid-phase peptide synthesis method. L-Alanyl-*D*-L-alanine ($NH_3C_{\alpha}DCH_3CONHC_{\alpha}HCH_3COOH$, AdA) and L-alanyl-*D*-L-alanine-*D* ($NH_3C_{\alpha}DCH_3CONHC_{\alpha}DCH_3COOH$, AdAd) were synthesized in Professor Max Diem's laboratory.¹⁸

Instrumentation. The UV Raman instrumentation is described in detail elsewhere.^{11,12,14,15} Most spectra shown were obtained using 206.5 nm excitation from a Coherent Inc. CW intracavity frequency-doubled Kr^{2+} laser.¹⁹ The Raman scattered light was collected in a $\sim 135^\circ$ backscattering geometry and dispersed by a Spex Triplemate monochromator. An intensified CCD detector (Princeton Instrument Co.) was used for detection. The samples were either measured as a stirred solution in a quartz cell or in a temperature controlled free-surface flowing stream.

Excitation at 204 nm was obtained by anti-Stokes Raman shifting the third harmonic of an Infinity YAG laser (Coherent Inc.) in H_2 .

(13) Chi, Z.; Chen X. G.; Holtz J. S. W.; Asher, S. A. *Biochemistry* **1998**, *37*, 2854–2864.

(14) Chen, X. G.; Li, P.; Holtz, J. S. W.; Chi, Z.; Pajcini, V.; Asher, S. A.; Kelly, L. A. *J. Am. Chem. Soc.* **1996**, *118*, 9705–9715.

(15) Li, P.; Chen, X. G.; Shulin, E.; Asher, S. A. *J. Am. Chem. Soc.* **1997**, *119*, 1116–1120.

(16) Chen, X. G.; Asher, S. A.; Schweitzer-Stenner, R.; Mirkin, N. G.; Krimm, S. *J. Am. Chem. Soc.* **1995**, *117*, 2884–2895.

(17) Lord, R. C. *Appl. Spectrosc.* **1977**, *31*, 187–194.

(18) Oboodi, M. R.; Alva, C.; Diem, M. *J. Phys. Chem.* **1984**, *88*, 501–505.

(19) Holtz, J. S. W.; Bormett, R. W.; Chi, Z.; Cho, N.; Chen, X. G.; Pajcini, V.; Asher, S. A.; Spinelli, L.; Owen, P.; Arrigoni, M. *Appl. Spectrosc.* **1996**, *50*, 1459–1468.

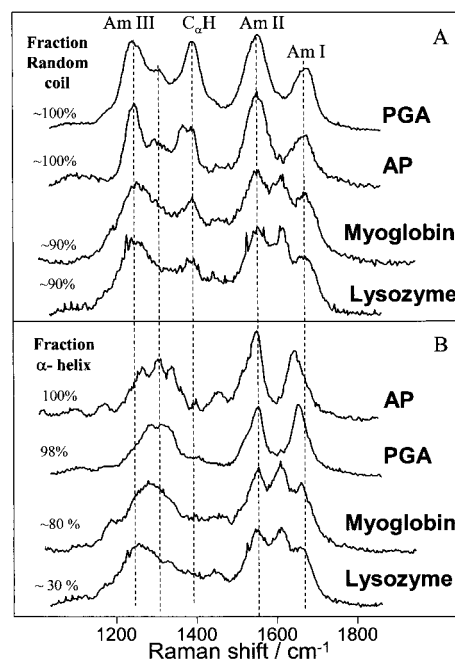


Figure 1. 204 nm excited UVRR spectra of polyglutamic acid (PGA), alanyl based peptide (AP), myoglobin, and lysozyme in their (A) random coil and (B) α -helical conformations. Experimental conditions (A) PGA: pH 7.1. AP: pH 7.0, 70 °C. Myoglobin: pH 4.0, 91 °C. Lysozyme: pH 2, 75 °C. (B) AP: pH 7, -5.5 °C. PGA: pH 4.31, 0 °C. Myoglobin: pH 4.0, 25 °C. Lysozyme: pH 2, 25 °C. The fractional α -helical and random coil contents indicated in the figure are from refs 12 and 13. We should note that the pH 7.1, 0 °C PGA sample is likely to also contain PPII type conformations (Tiffany, M. S.; Krimm, S. *Biopolymers* **1968**, *6*, 1379–1382. Keiderling, T. A.; Silva, R. A.; Dukor, R. K. *Bioorg. Med. Chem.* **1999**, *7*, 133–141. Barron, L. D. *J. Mol. Biol.* **2000**, *301*, 553–563.). We have not as yet characterized the UV Raman spectrum of the PPII conformation but expect the spectrum to be roughly similar to that of the β -sheet and random coil conformations because of the similarity in their ψ angles. We are further investigating this issue.

All spectra were normalized to the ClO_4^- internal standard band at 932 cm^{-1} . The broad 1640 cm^{-1} H_2O Raman bending band was subtracted using a measured solvent reference spectrum.

The CD spectra were measured by using a Jasco 710 spectropolarimeter.

Computation. The theoretical calculations were carried out using Gaussian 98W, revision A.9,²⁰ on a Dell 700 MHz Pentium III PC. The geometry optimizations and frequency calculations of alanine methylamide (AMA) were performed at the MP2 level of theory using the 6-31G(d) basis set. Variation of the ψ dihedral angle was carried out by first obtaining the global minimum energy conformation for alanine methylamide ($\psi = 146^\circ$). The minimum energy structure was then rotated to the required ψ dihedral angles (180, 120, 60, 30, 0, -60 , or -120°). This dihedral angle was fixed, the geometry was then reoptimized, and finally, the vibrational frequencies were calculated. The atomic displacement eigenvectors for the Am III and $(C)C_{\alpha}H$ modes were displayed using GaussView 2.1.

(20) Frisch, M. J.; Trucks, G. W.; Schlegel, H. B.; Scuseria, G. E.; Robb, M. A.; Cheeseman, J. R.; Zakrzewski, V. G.; Montgomery, J. A., Jr.; Stratmann, R. E.; Burant, J. C.; Dapprich, S.; Millam, J. M.; Daniels, A. D.; Kudin, K. N.; Strain, M. C.; Farkas, O.; Tomasi, J.; Barone, V.; Cossi, M.; Cammi, R.; Mennucci, B.; Pomelli, C.; Adamo, C.; Clifford, S.; Ochterski, J.; Petersson, G. A.; Ayala, P. Y.; Cui, Q.; Morokuma, K.; Malick, D. K.; Rabuck, A. D.; Raghavachari, K.; Foresman, J. B.; Cioslowski, J.; Ortiz, J. V.; Stefanov, B. B.; Liu, G.; Liashenko, A.; Piskorz, P.; Komaromi, I.; Gomperts, R.; Martin, R. L.; Fox, D. J.; Keith, T.; Al-Laham, M. A.; Peng, C. Y.; Nanayakkara, A.; Gonzalez, C.; Challacombe, M.; Gill, P. M. W.; Johnson, B. G.; Chen, W.; Wong, M. W.; Andres, J. L.; Head-Gordon, M.; Replogle, E. S.; Pople, J. A. *Gaussian 98*, revision A.9; Gaussian, Inc.: Pittsburgh, PA, 1998.

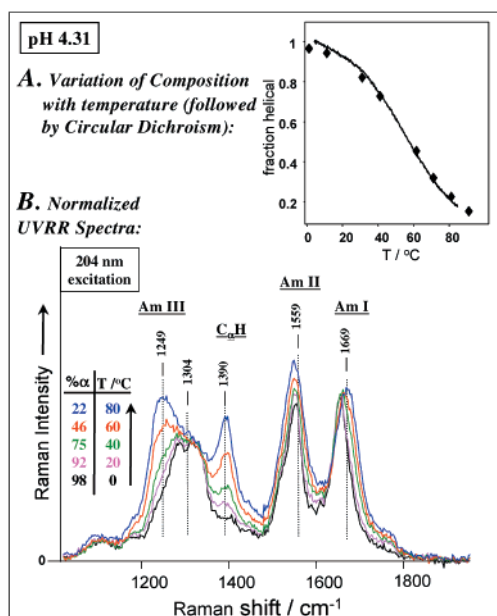


Figure 2. UVRR (204 nm) of α -helical and random coil forms of polyglutamic acid (PGA) at pH 4.31. (A) Dependence of the fractional α -helix on temperature as calculated from the CD spectrum. (B) Temperature dependence of the 204 nm excited UVRR of PGA during its thermal transition from $\sim 100\%$ α -helical at low temperature to almost pure random coil form at 80°C . α -Helical content was calculated using the method described in ref 13.

Results and Discussion

A. Conformational Dependence of Amide Bands of Peptides and Proteins. Figure 1 shows the strong conformational dependence of the 204 nm UV resonance Raman (UVRR) spectra of a series of peptides and proteins, while Figure 2 shows this conformational dependence for polyglutamic acid. These UVRR were excited within their ~ 200 nm amide $\pi \rightarrow \pi^*$ transitions, which gives rise to selective enhancement of the amide vibrations of the peptide backbone.¹⁶ The spectra are dominated by the Am I band ($1630\text{--}1680\text{ cm}^{-1}$), the Am II band (1550 cm^{-1}), the Am III band ($1240\text{--}1300\text{ cm}^{-1}$), and the $\text{C}_{\alpha}\text{H}$ bending band ($\sim 1400\text{ cm}^{-1}$). Additionally, the protein spectra show a contribution at $\sim 1600\text{ cm}^{-1}$ from the aromatic ring breathing vibrations of Tyr and Trp residues.¹³ Comparing Figures 1 and 2, we see that a change from a random coil to an α -helix conformation results in a small ($25\text{--}30\text{ cm}^{-1}$) downshift of the $\sim 1680\text{ cm}^{-1}$ Am I vibration and an even smaller downshift of the Am II band. Much more dramatic changes occur for the Am III and the $\text{C}_{\alpha}\text{H}$ bending bands; the Am III band upshifts from $\sim 1240\text{ cm}^{-1}$ to a broad band at $\sim 1300\text{ cm}^{-1}$ with a decreased peak intensity, while the $\sim 1400\text{ cm}^{-1}$ $\text{C}_{\alpha}\text{H}$ bending band disappears in the α -helix conformation. The $\sim 1300\text{ cm}^{-1}$ Am III band shape is broad and appears to show substructure, indicating overlapping vibrational bands.

Both the protein and polypeptide UVRR spectra show that the Am III and $\text{C}_{\alpha}\text{H}$ bending bands are the most conformationally dependent. The observed spectral structure correlation between a large Am III band frequency increase and the disappearance of the $\text{C}_{\alpha}\text{H}$ bending band hints at coupling between these motions. Further, the breadth of the Am III band suggests that this band has a complex origin.¹²

B. Origin of Resonance Raman Enhancement of the $\text{C}_{\alpha}\text{H}$ Bending Normal Mode. Enhancement of $\text{C}_{\alpha}\text{H}$ bending vibration upon excitation within the amide $\pi \rightarrow \pi^*$ transition is surprising, because the amide $\pi \rightarrow \pi^*$ transition excited-state

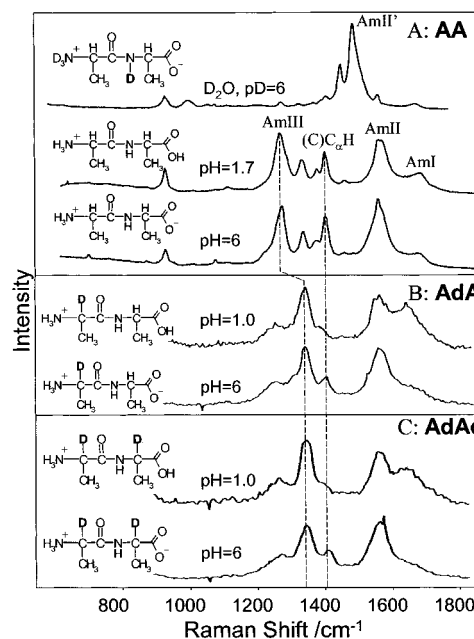


Figure 3. UV Raman spectra of various alanylalanine isotopomers: (A) alanylalanine (AA), D_2O , pD 6.0, pH 1.7, and pH 6.0, 5 mM, $\lambda = 206.5\text{ nm}$; (B) AA deuterated at the (C) C_{α} H position ($\text{H}_2\text{NC}_{\alpha}\text{DCH}_3\text{---CONHC}_{\alpha}\text{HCH}_3\text{COOH}$, AdA), pH 1.0, pH 6.0, 5 mM, $\lambda = 218\text{ nm}$; and (C) AA deuterated at the (C) C_{α} H and (N) C_{α} H positions ($\text{H}_2\text{NC}_{\alpha}\text{---DCH}_3\text{CONHC}_{\alpha}\text{DCH}_3\text{COOH}$, AdAd), pH 1.0, pH 6.0, 5 mM, $\lambda = 218\text{ nm}$. The AdA and AdAd pH 1.0 spectra have a contribution from the 1640 cm^{-1} H_2O bending band. The $\text{C}_{\alpha}\text{H}$ bending band at 1403 cm^{-1} only appears in the AA spectra.

distortion does not appear to have any projection along the $\text{C}_{\alpha}\text{H}$ bending coordinate.¹⁶ The observed enhancement of the peptide $\text{C}_{\alpha}\text{H}$ bending vibrations presumably results from the contribution of other amide atomic motions to the $\text{C}_{\alpha}\text{H}$ bending vibration. This mechanism explained the enhancement of the $\text{C}_{\alpha}\text{H}_3$ symmetric bending (sb) band of *N*-methylacetamide (NMA).¹⁶ The $\text{C}_{\alpha}\text{H}_3$ sb is enhanced within the amide $\pi \rightarrow \pi^*$ transition because of the contribution of $\text{C}_{\alpha}\text{---C}$ stretching. This requirement for enhancement of $\text{C}_{\alpha}\text{---C}$ stretching is especially clear in NMA, because the UVRR of methyl-deuterated NMA shows no enhancement of the ND_3 sb motion; it is almost a pure ND_3 sb vibration.

To obtain further information on the enhancement mechanism of $\text{C}_{\alpha}\text{H}$ bending vibrations, we investigated the enhancement of the two $\text{C}_{\alpha}\text{H}$ groups in a series of dipeptides. Figure 3 compares the pH 1.7 and pH 6 spectra of AA to those of its derivatives deuterated at the (C) C_{α} position (AdA) and to those deuterated at both the (C) C_{α} and (N) C_{α} positions (AdAd). The major differences between the low pH and neutral pH AA spectra derive from the enhancement of the low pH protonated carboxyl $\sim 1700\text{ cm}^{-1}$ carbonyl stretch and the pH 6 enhancement of the $\sim 1400\text{ cm}^{-1}$ symmetric carboxylate stretch.¹⁴ Thus, the Am III and the Am II band frequencies and relative intensities are independent of pH between pH 1.7 and 6, where AA shifts from the cationic to the zwitterionic forms.

AdA and AdAd show very similar spectra, while AA displays additional features. The AA spectrum shows at least two resonance enhanced Am III bands at 1270 and 1336 cm^{-1} which result from a complex mixing of NH ib (in plane bending), CN s, (C) C_{α} H b, and $\text{C}_{\alpha}\text{H}_3$ sb.^{18,21–27}

(21) Diem, M.; Oboddi, M. R.; Alva, C. *Biopolymers* **1984**, *23*, 1917–1930.

(22) Diem, M.; Lee, O.; Roberts, G. M. *J. Phys. Chem.* **1992**, *96*, 548–554.

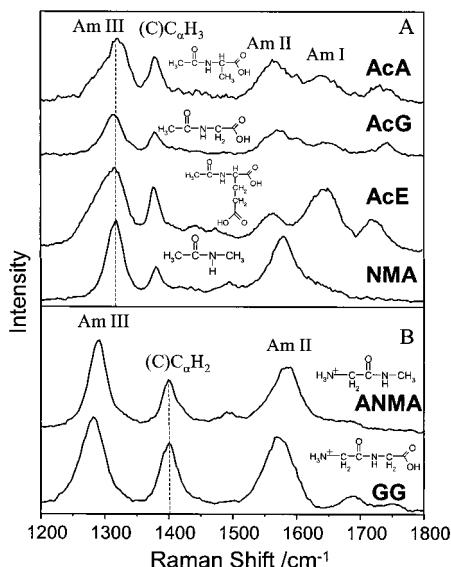


Figure 4. (A) 206.5 nm excited UV Raman spectra of different *N*-acylated dipeptides. The Am III band appears in *N*-acetyl-D-alanine ($\text{CH}_3\text{CONHCH}_2\text{COOH}$, AcA), *N*-acetyl glycine ($\text{CH}_3\text{CONHCH}_2\text{COOH}$, AcG), *N*-acetyl glutamic acid (AcE, $\lambda_{\text{ex}} = 244$ nm) (pH 1, 5 mM), and *N*-methylacetamide (pH 7, 5 mM). (B) Comparison between diglycine (5 mM, pH 1, GG) and C-terminal capped diglycine ($\text{NH}_3\text{-CH}_2\text{CONHCH}_3$, ANMA, 5 mM, pH 7). Only the (C) $\text{C}_\alpha\text{H}_2$ wagging band at 1400 cm^{-1} is resonant enhanced in the diglycine spectrum.

The C_αH band appears at 1403 cm^{-1} . The Am II and Am I bands occur at 1569 and 1684 cm^{-1} , respectively. These assignments are confirmed by AA spectra measured in D_2O , where exchange of N–H to N–D results in the disappearance of the Am III and Am II bands and the 1336 cm^{-1} band and in the formation of a very intense Am II' band. By comparing the spectra in Figure 3, it is clear that the 1403 cm^{-1} band must be due to a (C) C_αH group vibration, because it is absent in the AdA and AdAd spectra.

The spectra of AdA and AdAd are almost identical; they are dominated by a single 1338 cm^{-1} Am III band (slightly higher in AdAd), the 1570 cm^{-1} Am II band, and the 1654 cm^{-1} Am I band. The lack of bands in the $\sim 1400\text{ cm}^{-1}$ region for the deuterated derivatives indicates that the (N) C_αH b band in AA is not resonance enhanced by the amide $\pi \rightarrow \pi^*$ transition.

The lack of enhancement of the (N) C_αH bending appears to be quite general; previous studies of NMA demonstrated a lack of enhancement for the N– CH_3 sb vibration.²⁸ Figure 4 compares the pH 1 UVRR of NMA, acetylalanine (AcA), acetylglutamic acid (AcE), and acetylglycine (AcG), as well as glycyilmethylamide (ANMA) and glycyglycine (GG). Acetylation replaces the (NH₃) C_αH group with a methyl group which gives rise to the well-known $\sim 1380\text{ cm}^{-1}$ (C) CH_3 sb vibration.¹⁶ The Am III bands occur at $\sim 1320\text{ cm}^{-1}$, the Am II bands occur at $\sim 1565\text{ cm}^{-1}$, and the Am I bands occur at $\sim 1640\text{ cm}^{-1}$ in these spectra. These spectra exhibit a strong enhancement of (C) $\text{C}_\alpha\text{H}_3$ sb but no additional bands which would suggest enhancement of (N) C_αH b or (N) $\text{C}_\alpha\text{H}_2$ sb.

(23) Barron, L. D.; Gargaro, A. R.; Wen, Z. Q. *J. Chem. Soc., Chem. Commun.* **1990**, 1034–1036.

(24) Hecht, L.; Barron, L. D. *Faraday Discuss.* **1994**, 99, 35–47.

(25) Freedman, T. B.; Chernovitz, A. C.; Zuk, W. M.; Paterlini, M. G.; Nafie, L. A. *J. Am. Chem. Soc.* **1988**, 110, 6970–6974.

(26) Roberts, G. M.; Lee, O.; Calienni, J.; Diem, M. *J. Am. Chem. Soc.* **1988**, 110, 1749–1752.

(27) Weir, A. F.; Lowrey, A. H.; Williams, R. W. *Biopolymers* **2001**, 58, 577–591.

(28) Wang, Y.; Purello, R.; Jordan, T.; Spiro, T. G. *J. Am. Chem. Soc.* **1991**, 113, 6359–6368.

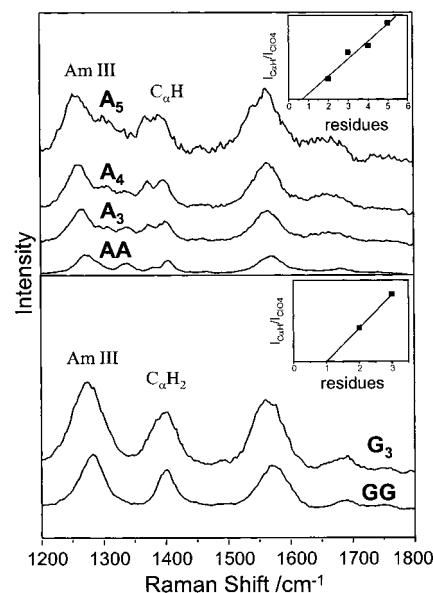


Figure 5. Upper panel shows the UV Raman spectra of alanylalanine (5 mM, AA), trialanine (1.5 mM, A₃), tetraalanine (1 mM, A₄), and pentaalanine (0.5 mM, A₅) at pH 1. The lower panel shows spectra of diglycine (5 mM, GG) and triglycine (1.5 mM, G₃) at pH 1. The C_αH bending band in the alanine based peptide spectra and the $\text{C}_\alpha\text{H}_2$ band in the glycine based spectra appear at $\sim 1400\text{ cm}^{-1}$. The inset, which shows the dependence of the integrated area of this band on the number of residue, indicates an intercept of one.

The pH 1 spectra of ANMA and GG show strong C_α methylene hydrogen bending vibrations at $\sim 1400\text{ cm}^{-1}$, while ANMA shows no evidence of the (N) CH_3 sb band. The relative intensity of the C_α methylene hydrogen bending bands is essentially identical for ANMA and GG, which also indicates a lack of enhancement of N–C methylene hydrogen bending. All of these results indicate that a lack of enhancement of (N)- C_αH bending vibrations is a general property of peptides.

This lack of enhancement of the (N) C_αH bending vibrations also occurs in larger peptides, as is evident from the Raman spectra shown in Figure 5 of AA, A₃, A₄, A₅, GG, and G₃ at pH 1. This is clearly evident in the insets to Figure 5, which show that the intensity of the (C) C_αH b band increases linearly with the number of alanine residues, but the intercept indicates that the penultimate (N) C_αH bending vibration shows no enhancement in these alanine peptides. A similar lack of enhancement for the carboxyl terminal (N) $\text{C}_\alpha\text{H}_2$ methylene hydrogen bending band is evident for G₃. Thus, we conclude that (N) C_αH bending or methylene hydrogen bending vibrations of the carboxyl-terminal residues of peptides are not enhanced in UVRR spectra excited within the amide $\pi \rightarrow \pi^*$ transitions.

The UVRR spectra of peptides are qualitatively different from spectra observed by other vibrational spectroscopies.^{18,21–27} For example, the UV resonance Raman spectra of AA in the $1200\text{--}1450\text{ cm}^{-1}$ region show only a few bands, while normal nonresonance Raman, VCD, and ROA spectroscopies show overlapping contributions of numerous bands in this very congested vibrational frequency region. The UV Raman spectra are dominated by the few vibrations which are Franck–Condon coupled to the amide $\pi \rightarrow \pi^*$ transition.¹⁶ In the case of AA, this is limited mainly to the Am III and the in plane (C) C_αH b. In contrast, the other vibrational spectroscopies not only show contributions of the bands observed in the UVRR but also out of plane (C) C_αH b, as well as in plane and out of plane (N)- C_αH bending,^{18,21,22} NH_2 bending, and the CH_3 umbrella modes. These other bands are weak or invisible in the UVRR. The

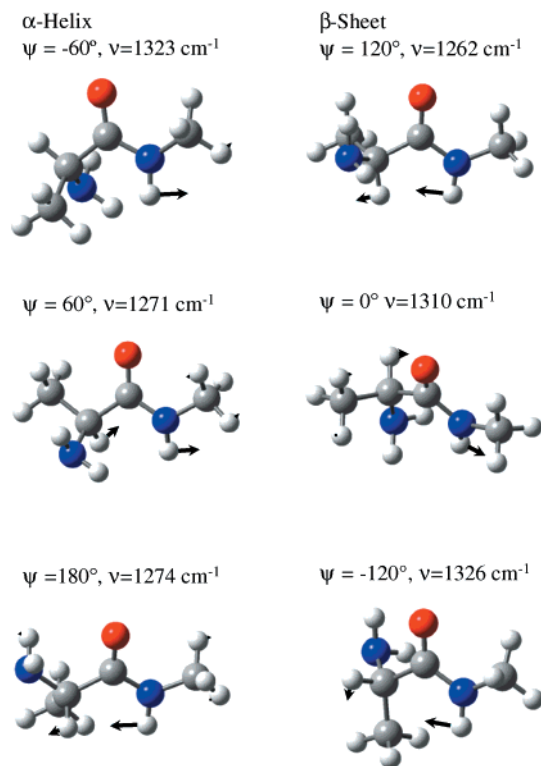


Figure 6. ψ angle dependence of the geometry and the Am III vibrational displacements as calculated by MP2 6-31G(d). Note that there is strong coupling of N–H and $C_{\alpha}H$ bending motions for conformations similar to that of the β -sheet ($\psi \sim 120^\circ$), but there is no coupling for α -helix conformations ($\psi \sim 60^\circ$).

difference in spectral contributions between UV Raman and the normal Raman, VCD, and ROA spectroscopies is most evident for the D_2O AA UVRR, where the Am III' band intensity is 10-fold larger than those for all other vibrations. The advantage of UV Raman measurements is that it fortuitously selects for the Am III and $(C)C_{\alpha}H$ b vibrations, which are especially sensitive to the peptide backbone conformation, as shown herein.

C. Conformational Dependence of the Am III and $(C)C_{\alpha}H$ Bending Vibrations Derives From Coupling Between N–H and $(C)C_{\alpha}H$ Bending. A detailed understanding of the peptide and protein UVRR conformational dependence requires a clear picture of which atomic motions give rise to the observed Raman bands and of how different secondary structure conformations determine the vibrational normal modes and their RR enhancement mechanisms. A cursory examination of the conformational dependence of the UVRR suggests a coupling between the Am III and the $(C)C_{\alpha}H$ sb vibrations. An examination of the amide geometry difference between the α -helix conformation, where $\psi = -60^\circ$, and the most likely random coil conformation ψ angle indicates a very large change in the interactions between $(C)C_{\alpha}H$ sb motion and the N–H bending motion associated with the Am III vibration (Figure 6).

As evident from the Ramachandran plot,²⁹ the random coil conformations will be dominated by ψ angles associated with β -sheet-like structures, $\psi \sim 120^\circ$. When $\psi \sim 120^\circ$, the $(C)C_{\alpha}H$ is in van der Waals contact with the N–H; any in plane Am III N–H motion must couple to $(C)C_{\alpha}H$ motion. In contrast, for the α -helix, the $(C)C_{\alpha}H$ is trans to the N–H, and no coupling should occur.

This hypothesis is consistent with previous normal mode calculations of peptides. For example, vibrational analysis of

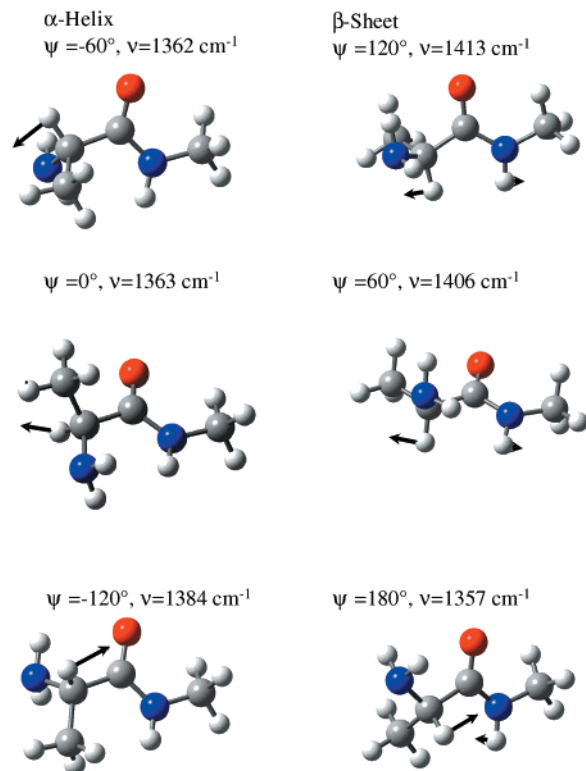


Figure 7. ψ angle dependence of the geometry and the $C_{\alpha}H$ bending vibrational displacements as calculated by MP2 6-31G(d). Note that there is strong coupling of N–H and $C_{\alpha}H$ bending motions for conformations similar to that of the β -sheet ($\psi \sim 120^\circ$), but there is no coupling for α -helix conformations ($\psi \sim 60^\circ$). The α -helix shows almost a pure $C_{\alpha}H$ bending vibration.

the crystalline tri-L-alanine β -structure shows that the Am III band is associated with a complex motion which involves N–H bending, CC s, CN s, and $C_{\alpha}H$ bending modes,³⁰ while the $(C)C_{\alpha}H$ bending motion is heavily mixed with N–H bending.³⁰ In contrast, normal mode calculations of α -helix polyalanine show an almost pure $(C)C_{\alpha}H$.³¹

To shed further light on the ψ angle dependence of the amide normal modes, we utilized Gaussian 98 to perform ab initio calculations at the MP2 6-31g(d) level of theory for AMA (i.e., $NH_2-CHCH_3-CONH-CH_3$) in a vacuum. Energy minimization yields a structure with a dihedral angle $\psi = 146^\circ$. This is close to the geometry of the C_5^{ext} conformation obtained for isolated AAMA by Han et al.³² We then used Gaussian 98 to find the minimum energy structure of conformations constrained to have the set of ψ -values: $\psi = -120^\circ$, -60° (α -helical), 0° , 30° , 60° , 120° (β -sheet), and 180° . We then performed normal coordinate calculations for each of these geometries.

Figure 6 shows the minimized geometries and vibrational displacements of the Am III modes for the different ψ dihedral angles, while Figure 7 shows the minimized geometries and vibrational displacements for the $(C)C_{\alpha}H$ bending modes. In agreement with our hypothesis, the Am III mode of the β -sheet conformation ($\psi = 120^\circ$) shows a very strong contribution from $(C)C_{\alpha}H$ bending; the $(C)C_{\alpha}H$ bending occurs in phase with N–H bending. The β -sheet Am III band is resonance enhanced by its large contribution of $C(O)-N$ stretching.¹⁶

(30) Qian, W.; Bandekar, J.; Krimm, S. *Biopolymers* **1991**, *31*, 193–210.

(31) Lee, S.-H.; Krimm, S. *Biopolymers* **1998**, *46*, 283–317.

(32) Han, W. G.; Jalkanen, K. J.; Elstner, M.; Suhai, S. *J. Phys. Chem. B* **1998**, *102*, 2587–2602.

(29) Creighton, T. E. *Proteins. Structure and molecular properties*, 2nd edition; W. E. Freeman and Company: New York, 1993; p 183.

In contrast, the Am III mode of the α -helix conformation ($\psi = -60^\circ$) shows little (C) C_α H bending but contains a large component of N–H bending (Figure 6). The α -helix conformation Am III band is resonance enhanced because it contains a significant contribution of an asymmetric C_α –C(O)–N stretching vibration. This motion gives rise to resonance Raman enhancement in a similar manner as in NMA.¹⁶

Similarly, the (C) C_α H bending mode of the β -sheet conformation (Figure 7, $\psi = 120^\circ$) shows strong mixing of N–H bending with (C) C_α H bending, while the α -helix ($\psi = -60^\circ$) conformer has essentially a pure C_α H bending vibration (except for a small contribution of C_α C(O) stretching). The β -sheet conformation shows an out of phase coupling of N–H and (C)– C_α H bending. This (C) C_α H bending band is enhanced, because it contains a significant contribution of an asymmetric C_α –C(O)–N stretching motion.

The elements of the Hessian matrices were calculated for AMA for ψ dihedral angles fixed at 120° and -60° . The diagonal elements, which are the force constants in internal coordinates for N–H bending, were found to be 0.260 120 hartree/rad² for $\psi = 120^\circ$ and 0.247 665 hartree/rad² for $\psi = -60^\circ$. For $\psi = 120^\circ$, close to the β -sheet conformation, the off-diagonal force constant between (C) C_α –H bending and N–H bending is 0.010 074 hartree/rad². In contrast, for $\psi = -60^\circ$, close to the α -helix conformation, the off-diagonal is 10-fold smaller ($-0.001 225$ hartree/rad²). These results show that strong vibrational coupling exists between the N–H bending and (C) C_α –H bending for the $\psi = 120^\circ$ conformation and that N–H/ C_α –H coupling is significantly reduced for $\psi = -60^\circ$. We should note that, while our paper was under review, Weir et al.²⁷ also noticed that a conformation of dialanine, where $\psi = 130^\circ$, shows a strong coupling of N–H in plane bending with (C) C_α H bending.

Figure 8A,B shows the calculated ψ angle frequency dependence of the Am III vibration and the (C) C_α H bending vibration. The Am III vibration shows an approximate $\nu = \nu_0 + A \sin \psi$ dependence, where $A \sim 61 \text{ cm}^{-1}$. Thus, we calculate a 61 cm^{-1} decreased frequency for the Am III band in the random coil and β -sheet conformations compared to that of the α -helix conformation, which is close to that observed in Figures 1 and 2. In fact, it is very close to the observed Am III frequency difference between AA and AdA (66.5 cm^{-1} , Figure 3); replacement of (C) C_α H with (C) C_α D would remove any (C)– C_α H bending contribution to the Am III vibration. According to our hypothesis, this would have the identical impact as altering the ψ angle such that the (C) C_α H and NH groups are trans, as in the α -helix conformation.

The (C) C_α H bending vibration shows a maximal frequency at $\psi = 120^\circ$ and a minimum for the $\psi = -60^\circ$, in the α -helix conformation. If the band were slightly enhanced by its component of C_α –C(O) stretching in the α -helix structure, it would probably begin to overlap the high-frequency side of the Am III band.

Our calculations have not yet examined the solvent dependence of the amide vibrational modes. While these studies are important, we expect to find little Am III solvent dependence, independent of the amide conformational alterations which impact the ψ angle. While the amide geometry could be solvent dependent,^{32–36} we observe only modest UV resonance Raman spectral changes for AA between water and a solution of 75% acetonitrile/25% water (data not shown). In fact, NMA shows similar Am III bands in water and pure acetonitrile.^{34–36}

(33) Deng, Z.; Polavarapu, P. L.; Ford, S. J.; Hecht, L.; Barron, L. D.; Ewig, C. S.; Jalkanen, K. *J. Phys. Chem.* **1996**, *100*, 2025–2034.

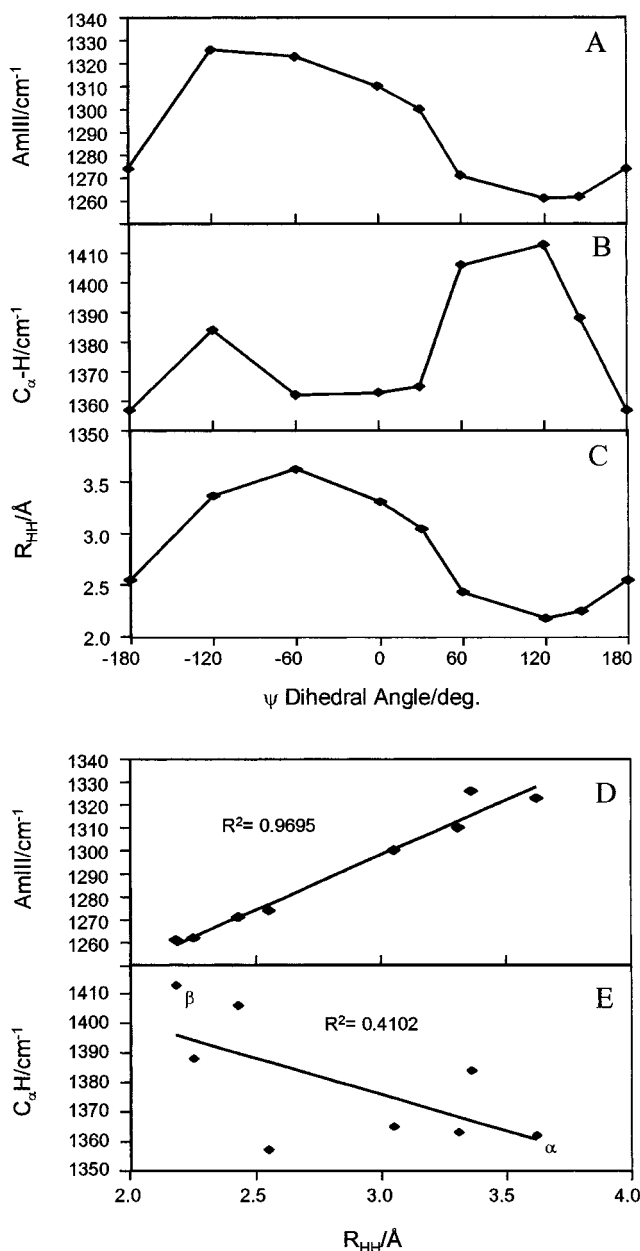


Figure 8. ψ dihedral angle dependence of the (A) Am III frequency; (B) C_α H bending vibration; and (C) the distance between the N–H and C_α H hydrogens, R_{HH} , as calculated by MP2 6-31G (d). (D) Dependence of the Am III frequency on R_{HH} . (E) Dependence of the C_α H bending vibrational frequency on R_{HH} .

N-Acetyl-*N'*-methyl-L-alaninamide (AAMA)³³ also shows similar normal Raman spectra in chloroform and water. Although AAMA shows a significant ROA solvent dependence for the Am I and Am II bands, little ROA dependence occurs for the Am III band.³³

D. Characterization of Vibrational Coupling. As shown in Figure 8D, the Am III band frequency varies linearly with the distance between the N–H and the (C) C_α H hydrogens, even at distances more than twice the hydrogen atom van der Waals radius (2.4 \AA). This dependence probably originates from the ψ angle dependence of the mutual projections of these bending motions. Figure 8E shows the dependence of the (C) C_α H

(34) Markham, L. M.; Hudson, B. S. *J. Phys. Chem.* **1996**, *100*, 2731–2737.

(35) Mayne, L. C.; Ziegler, L. D.; Hudson, B. *J. Phys. Chem.* **1985**, *89*, 3395–3398.

(36) Mayne, L. C.; Hudson, B. *J. Phys. Chem.* **1991**, *95*, 2962–2967.

bending vibrational frequency on the distance between the N–H and the (C)C $_{\alpha}$ H. There appears to be a calculated decrease in the frequency of the (C)C $_{\alpha}$ H bending vibration as the R_{HH} distance increases.

The 66.5 cm $^{-1}$ upshift of Am III of AA upon (C)C $_{\alpha}$ H deuteration is another strong indicator that the origin of the conformational dependence of the Am III and (C)C $_{\alpha}$ H b bands derives from coupling of (C)C $_{\alpha}$ H and N–H bending. We can utilize a simple coupled oscillator model to describe the interactions between the two almost degenerate modes. We begin by assuming for simplicity that, in the absence of coupling, Am III can be described as a vibration that contains mainly CC s, CN s, and NH b, while the (C)C $_{\alpha}$ H b is an isolated mode. In the presence of the coupling potential, V , these two modes mix, and their frequencies can be obtained by diagonalizing the Hamiltonian:³⁷

$$\hat{H}_c = \begin{pmatrix} \nu_{\text{CN,NH}} & V \\ V & \nu_{\text{CH}} \end{pmatrix} \quad (1)$$

where $\nu_{\text{CN,NH}}$ and ν_{CH} are the unperturbed frequencies of the Am III and the (C)C $_{\alpha}$ H bending motion. If the interaction potential V is expressed in units of reciprocal centimeters, eq 1 can be solved to yield the frequency difference $\Delta\nu$ due to the interaction potential V :

$$\Delta\nu = \sqrt{4V^2 + \Delta\nu_0^2} \quad (2)$$

where $\Delta\nu_0$ is the frequency difference from the unperturbed states. The spectra in Figure 3A,B show that elimination of the (C)C $_{\alpha}$ H b contribution shifts the Am III frequency by about half the original frequency difference between the undeuterated Am III band and the (C)C $_{\alpha}$ H b vibration. This indicates that $\Delta\nu_0 \approx 0$. Equation 2 estimates a coupling energy of $V = 66.5$ cm $^{-1}$. Thus, we expect that the splitting between the vibrations will increase as V increases. This is demonstrated by the calculations of Figure 8, which show that as the distances between the C $_{\alpha}$ H and N–H hydrogens increase the band frequencies move toward one another. We expect that the interaction potential will increase as the C $_{\alpha}$ H and N–H motions approach each other.

The linear distance dependence of NH–(C)C $_{\alpha}$ H coupling is surprising, as is the fact that this dependence continues even after the hydrogens are well out of van der Waals contact. The origin of this apparent linear dependence may simply be because the projection of the N–H and (C)C $_{\alpha}$ H bending motion on one another approximately follows a (sin ψ)-like dependence. Alternatively, the origin may be highly complex with different contributions occurring at different ψ angles.

Thus, our study here strongly supports Lord's early hypothesis that the Am III frequency depends on the dihedral angle ψ .¹⁷

(37) Herzberg, G. In *Molecular Spectra and Molecular Structure: II Infrared and Raman Spectra of Polyatomic Molecules*; Van Nostrand Reinhold Co.: New York, 1945; p 215–218.

The work here may lead to the realization of early studies by Peticolas et al.,³⁸ who, following Lord's¹⁷ suggestion, attempted to calculate the distribution of ψ angles in proteins from the measured Am III Raman band frequencies and bandwidths. Our Figure 8 results may in the future allow us to determine the ψ angle from the observed Am III and (C)C $_{\alpha}$ H bending frequencies.

To reach this goal, we will require information on the φ angle and the side chain dependences of the Am III frequency. It may even be possible to determine individual amide bond ψ angles. This is because the amide vibrations of peptides are often uncoupled, and the Raman spectra are a summation of independent contributions from each peptide bond.³⁹ We can straightforwardly determine both the Am III frequency and the (C)C $_{\alpha}$ H bending spectrum of each amide linkage by selectively deuterating the (C)C $_{\alpha}$ H moiety (Figure 3); the UV resonance Raman difference spectrum will display the required information.

We also must point out that in this work we have glossed over the complexity of the Am III Raman band shape and the detailed assignment of this (these) vibration(s). This issue will be discussed in detail in a separate report.⁴⁰

Conclusions

UV resonance Raman studies of peptide and protein secondary structure demonstrate an extraordinary sensitivity of the Am III vibration and the (C)C $_{\alpha}$ H bending vibration to the amide backbone conformation. We demonstrate that this sensitivity results from a Ramachandran dihedral ψ angle dependent coupling of amide N–H motion to (C)C $_{\alpha}$ H motion, which results in a ψ dependent mixing of the Am III and the (C)C $_{\alpha}$ H bending vibration. The vibrations are intimately mixed at $\psi \sim 120^\circ$, associated with both the β -sheet conformation and random coil conformations, but are essentially unmixed at $\psi \sim -60^\circ$ for the α -helix conformation. Theoretical calculations demonstrate a sinusoidal dependence of this mixing on ψ . These results explain both the Am III frequency dependence on conformation as well as the resonance Raman enhancement mechanism for the (C)C $_{\alpha}$ H bending vibration. These results may in the future allow us to extract amide ψ angles from measured UV resonance Raman spectra.

Acknowledgment. We thank Professors Sam Krimm, Igor Lednev, and Ken Jordan for numerous helpful conversations and acknowledge NIH Grant G.M.30741 for financial support. R.S.S. acknowledges support from the German Science Foundation (Schw 398/15-1), a NATO collaborative research grant (960030), and an EPSCOR-NSF grant.

JA0039738

(38) Peticolas, W. L.; Cutrera, T.; Rodgers, G. R. *Proc. Int. Symp. Biomol. Struct.* **1981**, *2*, 45–58.

(39) Mix, G.; Schweitzer-Stenner, R.; Asher, S. A. *J. Am. Chem. Soc.* **2000**, *122*, 9028–9029.

(40) Mix, G.; Schweitzer-Stenner, R.; Ianoul, A.; Boyden, M. N.; Asher, S. A. *J. Am. Chem. Soc.*, in preparation.